

Accepted Manuscript

Probabilistic online runoff forecasting for urban catchments using inputs from rain gauges as well as statically and dynamically adjusted weather radar

Roland Löwe, Søren Thorndahl, Peter Steen Mikkelsen, Michael R. Rasmussen, Henrik Madsen

PII: S0022-1694(14)00212-1

DOI: <http://dx.doi.org/10.1016/j.jhydrol.2014.03.027>

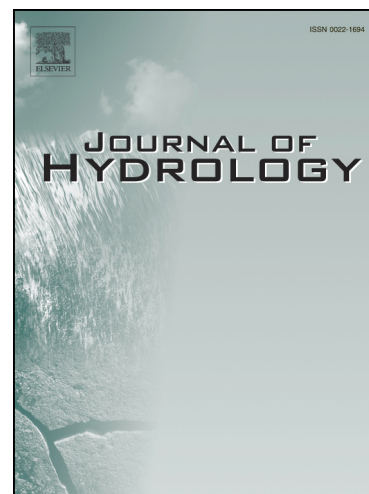
Reference: HYDROL 19485

To appear in: *Journal of Hydrology*

Received Date: 29 November 2013

Revised Date: 21 February 2014

Accepted Date: 10 March 2014



Please cite this article as: Löwe, R., Thorndahl, S., Mikkelsen, P.S., Rasmussen, M.R., Madsen, H., Probabilistic online runoff forecasting for urban catchments using inputs from rain gauges as well as statically and dynamically adjusted weather radar, *Journal of Hydrology* (2014), doi: <http://dx.doi.org/10.1016/j.jhydrol.2014.03.027>

This is a PDF file of an unedited manuscript that has been accepted for publication. As a service to our customers we are providing this early version of the manuscript. The manuscript will undergo copyediting, typesetting, and review of the resulting proof before it is published in its final form. Please note that during the production process errors may be discovered which could affect the content, and all legal disclaimers that apply to the journal pertain.

1 **Probabilistic online runoff forecasting for urban**
2 **catchments using inputs from rain gauges as well as**
3 **statically and dynamically adjusted weather radar**

4 Roland Löwe^{a,*}, Søren Thorndahl^c, Peter Steen Mikkelsen^b, Michael R. Rasmussen^c,
5 Henrik Madsen^a

6

7 *correspondence to: rolo@dtu.dk, +45-45253399

8 ^aDepartment of Applied Mathematics and Computer Science, Technical University of Denmark (DTU
9 Compute), Matematiktorvet B322, Kgs. Lyngby, 2800, Denmark, rolo@dtu.dk, hmad@dtu.dk

10 ^bDepartment of Environmental Engineering, Technical University of Denmark (DTU Environment),
11 Miljøvej B113, Kgs. Lyngby, 2800, Denmark, psmi@env.dtu.dk

12 ^cDepartment of Civil Engineering, Aalborg University, Sohngårdsholmsvej 57, Aalborg, 9000,
13 Denmark, st@civil.aau.dk, mr@civil.aau.dk

14

15 *ABSTRACT*

16

17 We investigate the application of rainfall observations and forecasts from rain gauges
18 and weather radar as input to operational urban runoff forecasting models. We apply
19 lumped rainfall runoff models implemented in a stochastic grey-box modelling
20 framework. Different model structures are considered that account for the spatial
21 distribution of rainfall in different degrees of detail.

22

23 Considering two urban example catchments, we show that statically adjusted radar
24 rainfall input improves the quality of probabilistic runoff forecasts as compared to

25 input based on rain gauge observations, although the characteristics of these radar
26 measurements are rather different from those on the ground. Data driven runoff
27 forecasting models can to some extent adapt to bias of the rainfall input by model
28 parameter calibration and state-updating. More detailed structures in these models
29 provide improved runoff forecasts compared to the structures considering mean areal
30 rainfall only.

31
32 A time-dynamic adjustment of the radar data to rain gauge data provides improved
33 rainfall forecasts when compared with rainfall observations on the ground. However,
34 dynamic adjustment reduces the potential for creating runoff forecasts and in fact
35 also leads to reduced cross correlation between radar rainfall and runoff
36 measurements. We conclude that evaluating the performance of radar rainfall
37 adjustment against rain gauges may not always be adequate and that adjustment
38 procedure and online runoff forecasting should ideally be considered as one unit.

39

40 *KEYWORDS*

41 Stochastic grey-box model, radar rainfall, radar adjustment, probabilistic forecasting,
42 real time control, urban hydrology

43

44 Received

45 2014/02/21

46

47

48 **1 INTRODUCTION**

49

50 Urban catchments are typically of a spatial extent where a homogeneous distribution
51 of rainfall over the catchment cannot be assumed. This is one of the main drivers for
52 developing real time control (RTC) setups for urban drainage systems. The load on
53 the sewer network is higher in some places than in others, which results in an uneven
54 use of the available storage capacities. This suboptimal load distribution can be
55 improved by a dynamic operation of the network. As a result, combined sewer
56 overflows can be reduced, for example.

57

58 Real time control systems are in operation in a multitude of urban catchments (Fuchs
59 and Beeneken, 2005; Pleau et al., 2005; Sharma et al., 2012, Seggelke et al., 2013).

60 Classically, decision making is done on the basis of offline knowledge about the
61 system, for example in a framework of decision rules. More recent developments
62 incorporate an online optimization of the system that accounts for runoff forecasts
63 (Puig et al., 2009; Vezzaro and Grum, 2012). The control setup suggested in Vezzaro
64 and Grum (2012) makes it possible to account for forecast uncertainties in the
65 optimization and decision making process.

66

67 In a dynamic optimisation based real time control setup, simplified rainfall runoff
68 models that lump a bigger part of the catchment are typically applied for forecasting
69 over short horizons of a few hours as they are fast enough to generate forecasts
70 within seconds to minutes (for example Pleau et al., 2001, Puig et al., 2009, Vezzaro
71 and Grum (2012)). Using highly simplified models for forecasting is also common in

72 other fields like district heating (Nielsen and Madsen, 2006) or wind power
73 forecasting (Giebel et al., 2011). Apart from being computationally efficient, lumped
74 models make the application of statistical techniques such as state-updating and
75 automated parameter calibration easier. Generating runoff forecasts in such an on-
76 line setup is the case we consider here.

77

78 Generating runoff forecasts on-line requires rainfall inputs. For forecast horizons up
79 to two hours, rainfall radars are currently the only means that provide the possibility
80 to generate rainfall forecasts with a spatial and temporal resolution suitable for urban
81 catchments. Examples of radar rainfall forecasting systems applied for quantitative
82 online predictions in urban drainage systems are rare (Einfalt et al., 2004), but can
83 for example be found in Einfalt et al. (1990), Kraemer et al. (2005) and Thorndahl
84 and Rasmussen (2013).

85

86 Emmanuel et al. (2012a) discourage the direct application of the French operational
87 weather radar product for quantitative purposes in urban hydrology. Similarly, other
88 authors propose an adjustment of radar data to rain gauge measurements (Thorndahl
89 et al., 2009; Villarini et al., 2010). Whereas the results of Villarini et al. (2010)
90 suggest a constant bias between radar and rain gauge measurements during an event,
91 other authors propose adjustment of radar measurements to gauge data also in the
92 course of an event (Borup et al., 2009; Brown et al., 2001; Chumchean et al., 2006;
93 Thorndahl et al., 2009, Wang et al., 2013, Wood et al., 2000). Gjertsen et al. (2003)
94 and Goudenhoofd and Delobbe (2009) give overviews of different methods applied
95 in Europe.

96

97 Radar adjustment is quite usually demonstrated to be beneficial by validating
98 adjusted radar observations against rain gauge observations (Goudenhoofdt and
99 Delobbe, 2009, Smith et al., 2007, Thorndahl et al., 2014, Wang et al., 2013) or by
100 generating runoff forecasts from models that were statically calibrated using rain
101 gauge input (Borup et al., 2009, Cole and Moore, 2008, Vieux and Bedient, 2004,
102 Wang et al., 2013). The improvement in runoff forecasting performance may
103 however be less clear for auto-calibrated online models that can dynamically adapt to
104 observations as well as different rainfall inputs. In such cases the skill of different
105 quantitative precipitation estimates to describe runoff should be assessed instead.
106 Gourley and Vieux (2005) follow this thought on a 1200 km² catchment to compare
107 results of spatially variable radar adjustments against mean field bias adjustment by
108 evaluating hydrologic simulation results with different rainfall inputs and ensembles
109 of different model parameters. They argue that rain gauge data may not be sufficient
110 for the validation of quantitative precipitation estimates (QPE) as they are often used
111 in the QPE algorithm itself, because rain gauge point measurements are often
112 inaccurate and because there are issues of different scales between rain gauges and
113 remotely sensed rainfall. The value of time varying radar adjustments for urban
114 online runoff forecasting is in our view unclear.

115

116 A second issue in the generation of online runoff forecasts is the required spatial
117 resolution of the rainfall input. A multitude of studies have been performed in
118 hydrology as to what degree of spatial model resolution is appropriate. The results
119 from the Distributed Model Intercomparison Project (Reed et al., 2004) show in a

120 non-urban context that conceptual models outperformed distributed models in the
121 majority of cases. Das et al. (2008) give an overview of studies and find that
122 generally, a higher spatial resolution does not necessarily lead to improved model
123 performance. The authors conclude that a multitude of factors like scale of the
124 catchment, physiographic characteristics or data availability influence model
125 performance and that a lower, optimal limit of spatial resolution is to be expected
126 because the model “represents spatial average behaviour”. This is underlined by
127 results obtained by the authors in predicting river discharge from a 4000 km²
128 catchment using different degrees of spatial resolution of model input data.
129
130 In urban hydrology, where catchment response is generally much faster than in
131 natural catchments and data typically available in higher resolutions, Schilling (1984)
132 and Schilling and Fuchs (1986) find that spatial rainfall variability is the key factor
133 for the accuracy of simulations of urban runoff and that rainfall estimation errors are
134 amplified by the rainfall runoff models. The authors suggest the use of high
135 resolution rainfall data and simplified models for on-line operations. Using a
136 hydrodynamic modelling setup for an 1100 ha catchment, Schellart et al. (2011)
137 conclude that spatial resolution of inputs should be high (in their case 1 km²) in order
138 to obtain a good representation of the observed flows in the sewer network. Finally,
139 Berne et al. (2004) suggest a spatial rainfall resolution of 3 km for a 1000 ha
140 catchment, while Emmanuel et al. (2012b) suggest 2.5 km resolution for a 600 ha
141 catchment and Schilling (1991) suggests 1 km for on-line purposes. Studies in urban
142 hydrology generally point in a direction where improved spatial resolution of rainfall
143 inputs leads to improved model performance, a result which is less clear in modelling

144 of river flows as the spatial scales considered are much larger and data more scarce.
145 We note that previous studies in urban hydrology focused on simulation, not on the
146 case of on-line runoff forecasting with models that adapt to observations, although
147 similar results may be expected.

148

149 Despite the above discussed results on model performance considering different
150 spatial resolutions of rainfall inputs, a practitioners approach to building an on-line
151 forecast model for real time control would often be to lump the catchment upstream
152 from a control point. Practical experience suggests that the effect of this lumping on
153 runoff simulation quality is limited (Achleitner et al., 2007; Grum et al., 2011; Wolfs
154 et al., 2013). Similar to previous studies in natural catchments (Das et al., 2008), we
155 therefore consider lumped models of different spatial resolutions for runoff
156 forecasting in urban catchments over short horizons.

157

158 Finally, runoff forecasts generated by any model are uncertain due to uncertain
159 measurements and forecasts of the rainfall input as well as an incomplete description
160 of the reality by the model. Achleitner et al. (2009) and Thorndahl and Rasmussen
161 (2013) evaluate the quality of urban runoff forecasts using radar rainfall input.
162 Acceptable forecast errors could be obtained for forecast horizons of 90 and 60
163 minutes, respectively. In an online setting, however, predicting also the uncertainty
164 of runoff forecasts is of strong interest. The performance of lumped rainfall-runoff
165 models in a stochastic grey-box layout was evaluated by Breinholt et al. (2011) and
166 Thordarson et al. (2012) but rainfall input was assumed known. We here present an

167 evaluation of probabilistic runoff forecast quality that can be obtained in a realistic
168 on-line setting.

169

170 Other approaches for modelling uncertainty in conceptual models exist and these
171 apply Bayesian frameworks (Del Giudice et al., 2013, Kuczera et al. 2006, Renard et
172 al., 2010), for example, GLUE (Breinholt et al., 2013, Dotto et al., 2012, Thorndahl
173 et al., 2008) or simple output error methods (Breinholt et al., 2012). The approach
174 presented here distinguishes itself in the explicit focus on forecasting over a
175 multitude of horizons on a short time scale instead of describing simulation
176 uncertainty and thus improving the capability of the model to describe reality. In
177 addition, high computational efficiency is a focus of the presented approach.

178

179 In the following, the article first gives an introduction to the rainfall data considered
180 as input for runoff forecasting in this study. Rainfall observations and forecasts from
181 rain gauges and two types of C-band radar data are evaluated and compared. The
182 types of weather radar data considered are

- 183 • temporally and spatially constant adjustment over the whole period (static
184 adjustment)
- 185 • time-dynamic mean-field bias adjusted to rain gauge measurements in the
186 course of an event, in addition to the static adjustment (dynamic adjustment).

187 The purpose of this evaluation is to demonstrate how the different rainfall
188 measurements relate to each other and that the dynamic adjustment indeed makes the
189 radar observations resemble the ground measurements more closely.

190

191 Subsequently, the different rainfall measurements and forecasts are considered as
192 inputs for runoff forecasting. A quantification of probabilistic online runoff
193 forecasting skill is provided on a 100 minute horizon. We evaluate if runoff forecasts
194 can be improved by the different types of radar rainfall input and by an increased
195 spatial resolution of the forecast model.

196

197 The article is structured as follows: section 2 describes the considered catchments,
198 available rainfall measurements, the methodology for generating and evaluating
199 stochastic runoff predictions, and the different model layouts considered. In section 3
200 we compare the available rainfall measurements from gauges and radar in the area,
201 and evaluate the runoff forecast quality obtained with different rainfall inputs and
202 model layouts. Finally, in section 4 we conclude the article.

203

204 **2 MATERIAL AND METHODS**

205 **2.1 CATCHMENTS**

206

207 Two catchments in the Copenhagen area are considered in this study. The Ballerup
208 catchment has a total area of approximately 1,300 ha. It is mainly laid out as a
209 separate sewer system but has a small combined part and shows strong influences
210 from rainfall-dependent infiltration and misconnection of surface runoff to sanitary
211 sewers (Breinholt et al., 2013).

212

213 The Damhusåen catchment is located close to Ballerup but drains to a different
214 treatment plant. We consider the northern part of the catchment with a total area of

215 approximately 3,000 ha. The catchment is laid out as a combined sewer system and
216 consists of several subcatchments with a longest flow path of approximately 10 km.

217

218 An overview of the catchments can be seen in Figure 1. Flow measurements
219 averaged over 5 min are available at the outlets of both catchments. Flow predictions
220 are generated for both outlets and compared to the observations at 10 min resolution,
221 where the measurements within an interval are averaged.

222

223

224 FIGURE 1 APPROX. HERE

225

226

227 **2.2 RAINFALL MEASUREMENTS AND FORECASTS USING GAUGES AND RADAR**

228 Observations from tipping bucket rain gauges from the Danish SVK network
229 (Jørgensen et al., 1998) are available in the considered catchments. Rainfall
230 measurements are available at 1 min intervals and averaged to 10 min time steps
231 (equivalent to the temporal resolution of the radar data). In the rain gauge based
232 forecast models we use 2 and 4 gauges as input for the Ballerup and Damhusåen
233 catchments (Figure 1). The gauges are located within or close to the catchment
234 borders.

235

236 Rainfall forecasts are generated from the gauge measurements using a local linear
237 trend method. A trend line is fitted to the rain gauge intensities in the past 100 min
238 and then extrapolated over the forecast horizon.

239

240 The Danish weather service operates a C-band radar in Stevns approx. 45 km south
241 of the considered catchments (Gill et al., 2006). Measurements from this radar were
242 made available for this study with a resolution of 10 min and $2 \times 2 \text{ km}^2$. Figure 1
243 shows the location of the catchments within the utilized C-band radar pixels.

244

245 We apply radar rainfall forecasts with lead times up to 100 min generated by Aalborg
246 University using the CO-TREC algorithm (Thorndahl and Rasmussen, 2013).

247 Corresponding to the available temporal resolution of the radar data, we apply all
248 rainfall input data with a temporal resolution of 10 min. Considering the spatial
249 extent of the catchments and concentration times t_c above 60 min, this resolution can
250 be considered sufficient to capture the rainfall runoff process in the catchments.

251 Schilling (1991) suggests a temporal resolution of the rainfall data which is between
252 $0.2t_c$ and $0.33t_c$.

253

254 **2.3 RADAR RAINFALL ADJUSTMENT**

255 C-band radar measurements are provided as reflectivities. A direct conversion to rain
256 intensities is commonly considered problematic. A methodology to adjust the radar
257 measurements to gauge observations has therefore been developed at Aalborg
258 University and is applied here.

259

260 In the adjustment, the rain gauges marked in Figure 1 are used (SVK numbers 30252,
261 30309, 30313, 30316, 30319, 30326, 30348 and 30386). The adjustment is
262 performed with only 8 gauges distributed in the Copenhagen area, as one of the main

263 objectives for using radar rainfall measurements is to derive rain intensities using as
264 small a number of ground measurements as possible.

265

266 In a first ‘static’ adjustment step, the coefficients in the reflectivity (Z) – rain
267 intensity (R) relationship are adjusted for the whole data period (see Section 2.4).

268 The rainfall depths from all rain events at all considered rain gauges are plotted
269 against the rainfall depths derived from the radar observations in the corresponding
270 pixels. The Z - R coefficients are adjusted, such that the regression line between radar
271 rainfall depths and rain gauge observations has slope 1 (Thorndahl et al., 2010). The
272 resulting Z - R relationship is used for deriving rain intensities over the whole data
273 period.

$$Z = 50 \cdot R^{1.8} \quad (1)$$

274

275 In a second ‘dynamic’ adjustment step, the radar rain intensities are again adjusted,
276 this time at every 10 min time step (Thorndahl et al., 2014). Considering the last 4
277 observations, a spatially constant adjustment factor is derived, such that the radar
278 measurements on average match the rain gauge measurements in the considered area.
279 This is a mean field bias adjustment in the sense of Goudenhoofd and Delobbe
280 (2009), however, with an adjustment window of 40 minutes instead of one day.

281

282 When generating forecasts, the time-dynamic adjustment factor is, over a period of
283 120 minutes, linearly changed to 1 with increasing lead time. The linear transition
284 towards zero-bias is performed because unrealistic and biased rainfall forecasts have

285 been observed on the longer lead times when forecasting with a time-dynamic
286 adjustment factor based on only the past 40 minutes.

287

288 **2.4 DATA PERIOD**

289 We use a summer period of 2.5 months from 25/06/2010 until 6/09/2010 for
290 generating probabilistic runoff forecasts. Figure 2 shows rain gauge and flow
291 observations from the Ballerup catchment for this period. We can clearly identify the
292 diurnal dry weather variations and a number of rain events that can be considered
293 relevant for real time control purposes. The measurements contain no major gaps in
294 this period.

295

296 FIGURE 2 APPROX. HERE

297

298

299 **2.5 STOCHASTIC FLOW FORECASTING**

300 **2.5.1 General Model Layout**

301 As mentioned before, we use stochastic grey-box models to generate flow forecasts
302 for the catchments. In the basic setup we use a linear reservoir cascade of 2 storages
303 with one rainfall input, implemented as stochastic differential equations in a state-
304 space model layout (Breinholt et al., 2011). The model is at every time step updated
305 to current flow observations using an extended Kalman filter (Kristensen et al.,
306 2004).

307

308 This setup has been extensively tested for the Ballerup catchment but not for the
 309 Damhusåen catchment. The model is obviously too simple, especially for the
 310 (bigger) Damhusåen catchment. As we are mainly interested in investigating the
 311 effects of different rainfall inputs on the forecasts, we still apply this most simple
 312 setup. With respect to the magnitude of runoff forecast uncertainties, this could be
 313 considered a ‘worst case scenario’.

314

$$d \begin{bmatrix} S_{1,t} \\ S_{2,t} \end{bmatrix} = \begin{bmatrix} A \cdot P + a_0 - \frac{1}{K} S_{1,t} \\ \frac{1}{K} S_{1,t} - \frac{1}{K} S_{2,t} \end{bmatrix} dt + \begin{bmatrix} \sigma_1 \cdot S_{1,t}^{\gamma_1} \\ \sigma_2 \cdot S_{2,t}^{\gamma_2} \end{bmatrix} d\omega_t \quad (2)$$

$$Q_k = \frac{1}{K} S_{2,k} + D_k + e_k \quad (3)$$

315

316 (2) is called the system equation, where S_1, S_2 correspond to the storage states, A to
 317 the impervious catchment area, P to the rain intensity, a_0 to the mean dry weather
 318 flow and K to the travel time constant. The uncertainty of model predictions is
 319 described in the so-called diffusion term by a Wiener process ω_t . The increments $d\omega_t$
 320 of this process are independent and normally distributed with a standard deviation
 321 corresponding to the considered time interval dt .

322

323 The variance of the diffusion is here scaled dynamically depending on the current
 324 model states S and a scaling factor σ . Such a scaling can be problematic for the
 325 extended Kalman filtering. A Lamperti transform is therefore applied that removes
 326 the state-dependency from the diffusion term and leads to a set of transformed drift

327 equations that equivalently describe the dynamics of the system, but have constant
328 diffusion (Breinholt et al., 2011).

329

330 States and flow measurements are related in the observation equation (3). Q_k
331 corresponds to the observed flow values at times k , D describes the variation of the
332 dry weather flow using trigonometric functions and e corresponds to the observation
333 error with standard deviation σ_e .

334

335 We refer to Kristensen et al. (2004) and Breinholt et al. (2011, 2012) for a detailed
336 description of the modelling principles. We use the open-source software framework
337 CTSM for the modelling process (Kristensen and Madsen, 2003).

338

339 **2.5.2 Stochastic Model Layout and Rainfall Inputs**

340 To investigate the influence of spatial resolution of rainfall inputs on the ability to
341 create stochastic runoff forecasts, we consider the following model layouts:

- 342 • Area mean – the rainfall is assumed constant over the whole catchment and
343 inputs from gauges or radar pixels are averaged (as shown in equation (2)).
- 344 • Integrated subcatchment – for radar inputs, the catchment is divided into
345 subcatchments (Figure 1), an impervious area is estimated for every
346 subcatchment, but only one storage cascade is used and all inputs are fed into
347 the first storage. The same approach is applied for rain gauge input, but we
348 estimate an effective area for every rain gauge and perform no assignment to
349 subcatchments. This approach is applied for the (smaller and less complex)
350 Ballerup catchment.

351 • Distributed subcatchments – every subcatchment has a cascade of 2 storages
352 of its own and the outflows from the northern and eastern subcatchments are
353 inputs to the western subcatchment. This approach is applied for the (bigger
354 and more complex) Damhusåen catchment. In the simulation run with rain
355 gauges, these are assigned to the closest subcatchment.

356

357 As a variety of rainfall inputs and model layouts are considered, in the following we
358 denote the different simulation runs with a 3-letter identifier in accordance with
359 Figure 3.

360

361

FIGURE 3 APPROX. HERE

362

363

364 **2.6 PARAMETER ESTIMATION**

365 Parameters for the proposed stochastic rainfall runoff models are estimated in an
366 automated optimization routine. Most commonly this is done by maximizing the
367 likelihood of one-step-ahead model predictions (Breinholt et al., 2011). In an online
368 setup, however, the models are intended to provide multistep predictions. The model
369 identified by minimizing the error of one-step-ahead predictions may not be the best
370 model in terms of forecasting with longer lead times.

371

372 Further, if there is strong noise on the flow observations, the model may not be
373 identifiable. The model setup includes a Kalman filtering procedure, which means
374 that the model states are updated to follow the observations at each time step. If the

375 model is estimated on the basis of one-step-ahead predictions, there is a risk that the
376 estimated model parameters simply optimize this state-updating and do not describe
377 the physical behaviour of the system.

378

379 We therefore here apply a parameter estimation method that minimizes the error of
380 the probabilistic multistep flow predictions (Löwe et al., 2014). The according
381 criterion is the continuous ranked probability score (*CRPS*). At every time step, this
382 score measures the squared difference between the cumulative distribution function
383 (CDF) of the forecast and the CDF of the observation, where the latter is considered
384 as a unit step at the observed value (Gneiting et al., 2005; Gneiting, 2007).

385

386 The dry weather parameters a_0 and D of the model are assumed fixed and are
387 estimated deterministically in a dry weather period of one week at the beginning of
388 the considered time series. We apply a heuristic optimization algorithm described by
389 Tolson and Shoemaker (2007) for automated parameter estimation.

390

391 **2.7 ON-LINE RUNOFF FORECAST GENERATION AND EVALUATION**

392 We evaluate the quality of probabilistic forecasts of runoff volume obtained from the
393 different models. Runoff volumes are the relevant decision variable in a real time
394 control setup for urban drainage systems as described e.g. by Vezzaro and Grum
395 (2012). To obtain probabilistic predictions of runoff volume, we do at every time
396 step generate 1000 realizations of multistep flow predictions from the model
397 equations (2) using an Euler Maruyama scheme (Kloeden and Platen, 1999). We
398 consider forecast horizons up to 10 steps or 100 min.

399

400 In this approach, forecast uncertainties are in the on-line setting only determined by
401 the state uncertainties, not the observation uncertainties. This is reasonable as in a
402 real time control scheme we are not interested in the observation uncertainty. The
403 estimated observation uncertainties are furthermore small compared to the
404 uncertainties of the model predictions (c.f. section 3.3).

405

406 Each of the 1000 multistep flow prediction scenarios can be integrated into a runoff
407 volume prediction. We can then analyse the distribution of these values to obtain an
408 empirical description of the predictive distribution of runoff volumes for each
409 horizon. We evaluate the quality of the 10-step probabilistic runoff volume
410 predictions as compared to the observed runoff volumes for this horizon. We
411 consider the following criteria:

- 412 • Reliability (*Rel*) – percentage of observations included in a 90% prediction
413 interval. Ideally, this value corresponds to 90%, higher values suggest an
414 overfitted model, lower values an unreliable model.
- 415 • Average Interval Length (*ARIL*) – average width of the 90% prediction
416 interval relative to the observations (Jin et al., 2010).
- 417 • Continuous ranked probability score (*CRPS*) – mean squared error of the
418 predictive runoff volume distribution for a 10-step horizon. The best forecast
419 minimizes this value (Gneiting, 2007).
- 420 • Root mean squared error (*RMSE*) between the 50% quantile of probabilistic
421 runoff volume predictions and the corresponding observation.

422

423 3 RESULTS AND DISCUSSION

424 3.1 COMPARING RADAR AND RAIN GAUGE OBSERVATIONS AND FORECASTS

425 In a first step, the different rainfall observations are compared. The considered data
426 period is split into rain events. Based on the spatially averaged rain gauge
427 observations, it is assumed that a new event starts after 10 hours of dry weather.
428 Rainfall intensities below 0.2mm/10min are considered dry weather and we only
429 consider events with a total rainfall sum of at least 5 mm.

430

431 Based on the above considerations, 10 rain events are identified from the averaged
432 rain gauge observations in the Ballerup catchment and used for comparison. Figure 4
433 shows the total rainfall depth and the maximum intensity together with the duration
434 of the events.

435

436 FIGURE 4 APPROX. HERE

437

438 The effect of the dynamic radar adjustment clearly varies from event to event. Yet,
439 on average, the root mean squared error (*RMSE*) between the total areal rainfall sums
440 measured by radar and rain gauges is reduced from 9.8 mm with the static
441 adjustment, to 7.3 mm for the dynamic adjustment. In the Damhusåen catchment (not
442 shown) similar results are obtained with a reduction of the *RMSE* from 11.0 mm for
443 the static adjustment to 6.7 mm for the dynamic adjustment.

444

445 Figure 5 supports the indications from the analysis of total rainfall sums. The
446 dynamically adjusted radar observations seem to better capture the rainfall dynamics

447 observed on the ground. However, in both cases, the radar rainfall forecasts fail to
448 predict the intense rainfall peak towards the end of the event. A delay is observed for
449 the rainfall forecasts derived from the gauge measurements. This is induced by the
450 forecast method which is based on extrapolating the observations of the last 100 min.

451

452 FIGURE 5 APPROX. HERE

453

454 Figure 6 shows the total rainfall sum for the different events derived from forecast
455 values for a 2-step (20 min) and a 10-step (100 min) horizon. The simplistic forecast
456 applied for the rain gauge data leads to a systematic overestimation of the total
457 rainfall. The forecasts generated from the dynamically adjusted radar data are close
458 to the rain gauge observations for the shorter horizon and approach the value for the
459 statically adjusted data on the longer horizon. This is in accordance with the radar
460 adjustment and forecasting methodology described in section 2.3.

461

462 FIGURE 6 APPROX. HERE

463

464 In Figure 4 one rain event can be identified (event 2) which is only present in the
465 gauge measurements but not in the radar measurements for the Ballerup catchment.

466 This deviation is a result of the gauges being located outside the catchment.

467

468 **3.2 CORRELATION BETWEEN RAINFALL AND RUNOFF OBSERVATIONS**

469

470 Figure 7 shows the estimated cross correlation between catchment averaged rainfall

471 observations and the measured runoff in the Ballerup catchment. For all rainfall

472 inputs, the highest cross correlation is identified for a lag of 16 time steps or 160
473 minutes. The highest correlation between rainfall and runoff measurements is
474 identified for statically adjusted radar measurements, and it is noticeably smaller for
475 dynamically adjusted radar measurements. The same result is obtained in the
476 Damhusåen catchment (not shown). It indicates that the type of time varying radar
477 adjustment as described in section 2 may actually reduce the information about the
478 runoff process that is contained in the radar rainfall time series. This is in spite of the
479 fact that the time varying adjustment makes the radar data resemble the rainfall
480 measurements on the ground more closely as described above.

481

482

FIGURE 7 APPROX. HERE

483

484 **3.3 PROBABILISTIC RUNOFF FORECASTING WITH DIFFERENT RAINFALL**

485

INPUTS

486 We consider the quality of probabilistic runoff forecasts obtained using mean areal
487 rainfall input derived from rain gauges and weather radar (model type a). Table 1
488 shows the effective catchment area and the time constant estimated for the different
489 models. We observe a tendency to estimate higher effective area values for the
490 models with statically adjusted radar rainfall input. This is likely to be a result of the
491 lower rain intensities in this type of input data (Figure 5).

492

493 Table 1. Estimated travel time constant (K) and impervious catchment area (A) for

494 mean areal rainfall models (type a) with rain gauge (1) and statically (2) and

495 dynamically (3) adjusted radar input for Ballerup (B) and Damhusåen (D)
 496 catchments.

Model	K [h]	A [ha]
B1a	4.62	70.6
B2a	4.50	74.4
B3a	3.79	61.4
D1a	2.01	278.3
D2a	4.45	392.1
D3a	4.66	253.4

497

498

499 Table 2 and Table 3 summarize the runoff forecast skill of the different models
 500 averaged over all 10 events. We see that all models seem to be rather unreliable, with
 501 only 51% to 72% of the observations included in a 90% prediction interval during
 502 rain periods. Considering the whole data period, including dry weather periods, 84 to
 503 92 % of the observations are included in a 90 % prediction interval (not shown).
 504 During dry weather periods, the flows in the sewer system are low and follow the
 505 well-defined diurnal cycle. The forecast error made by the runoff forecasting model
 506 is thus much smaller than during rain events. The uncertainty description in the
 507 model, however, accounts for dry and wet weather uncertainty in only one parameter.
 508 Uncertainties during rain events are hence forecasted too small. A solution to this
 509 problem could be to include a separate parameter for dry weather uncertainty in the
 510 diffusion term of equation (2).

511

512 We further identify an insufficient quantification of forecast uncertainties, in
 513 particular at the start of rain events (Figure 8). The reason is the state dependent

514 uncertainty description in the model, which only leads to high forecast uncertainties
515 for high forecast values. Ideally, the forecast uncertainty should increase already at
516 the start of the event. This may be achieved by conditioning the forecast uncertainty
517 on the rainfall input instead of the state values, but it is not further investigated here.

518

519 The models with statically adjusted radar rainfall input (input type 2) perform best in
520 both catchments and all model variations in matters of *RMSE*, whereas the models
521 with dynamically adjusted radar rainfall input result in higher *RMSE* values (Table 2 and Table 3). The forecast uncertainties for the radar based models are in
522 most cases estimated smaller. During rain periods, this leads to a more pronounced
523 underestimation of forecast uncertainties, resulting in some cases in a lower
524 probabilistic forecasting skill expressed as *CRPS*.

526

527 The better quality of runoff forecasts obtained with statically adjusted radar rainfall
528 input as compared to dynamically adjusted radar rainfall input seems to somewhat
529 contradict the results obtained by Borup et al. (2009). The authors showed that a
530 dynamic calibration of X-band radar rainfall measurements results in better
531 simulations of water levels at an overflow weir than a static calibration. Apart from
532 using a different type of radar rainfall measurements in this work, we see the main
533 reason for the differing results in the applied type of rainfall-runoff model and the
534 way radar forecasts are generated. A distributed simulation model was applied in the
535 work of Borup et al. (2009). These models are typically statically calibrated to reflect
536 observations in the sewer system based on rain gauge input. The model parameters
537 modified during the calibration (for example impervious area, surface roughness

538 values, pipe roughness values) do then also reflect the characteristics of rain gauge
539 input (for example higher intensities as compared to radar rainfall measurements).
540 Radar rainfall observations will consequently give better results the better they
541 reflect the rainfall measurements on the ground, but different results may be obtained
542 if the model is calibrated using radar rainfall input.

543

544 The rainfall runoff models applied in this work are data driven and fitted to the
545 supplied input data. The rainfall input for this type of model may well be biased as
546 compared to the “ground truth”, as the bias can be compensated for by different
547 parameter estimates (for example the impervious catchment area) and by the state
548 updating. The best runoff forecast will with this type of model be obtained with the
549 rainfall input that has the highest ‘information content’ with respect to the runoff
550 observations. This is the statically adjusted radar input in our case which is
551 underlined by the fact that this type of rainfall measurement shows the highest cross
552 correlation with the runoff time series.

553

554 More generally, it is interesting that the dynamically adjusted radar data appear to
555 provide less information about the runoff time series than both, the rain gauge and
556 the statically adjusted rainfall data. This is the case, not only for the radar rainfall
557 forecasts, but also for the radar rainfall measurements (see the cross correlation
558 function in Figure 7).

559

560 One likely reason is that the adjustment window of 40 minutes may be too short,
561 leading to a nonlinear alteration of the radar data which cannot be compensated for

562 by the automatic calibration of the rainfall-runoff model. This effect may be
563 amplified by the fact that radar rainfall measurements are made as ‘snapshots’ every
564 10 minutes, while the rain gauge data used for radar adjustment are continuous over
565 the interval. Recent works by Nielsen et al. (2014) and Thorndahl et al. (2014)
566 suggested an interpolation of the radar data to a higher temporal resolution using an
567 advective model and demonstrated that such processing reduces the bias as compared
568 to rain gauge measurements. The effect of such interpolation schemes on on-line
569 runoff forecasts needs to be investigated. In general, we suggest that the development
570 of an adjustment methodology focuses not only on the deviation between radar
571 rainfall estimates and rain gauges but also on the information content about the
572 runoff time series.

573

574 Additionally, when generating rainfall forecasts, the bias between the dynamically
575 adjusted radar forecast that is considered here and the observation on the ground
576 changes linearly as a function of the forecast horizon. The reason is that especially in
577 situations with sparse or very inhomogeneous rainfall within the radar range we risk
578 adjusting the mean field based on very few radar-rain gauge pairs with very little
579 observed rain. This might result in very small or very large adjustment factors.

580 Applying these adjustment factors to the forecast has previously produced severe
581 over- or underestimation of the forecasted rain. More rain gauges within the range of
582 the radar might reduce the problem but would also reduce the added value of the
583 radar. Generally, the non-constant bias in the rainfall forecasts introduces additional
584 uncertainty in the runoff forecast. Improved results can likely be obtained if

585 replacing the simple linear change of the bias factor by time series models that are
 586 fitted in a way such that the runoff forecast error is minimized.

587

588 Table 2. Forecast evaluation for mean areal rainfall (type a) and integrated
 589 subcatchment (type b) models with different rainfall inputs for the Ballerup
 590 catchment (B). Values are based on predicted runoff volumes in m^3 over a prediction
 591 horizon of 100 min (10 time steps) and averaged over the considered rain events. We
 592 include RMSE values for 1-step and 10-step prediction horizons.

Model	Rel [%]	ARIL [%]	CRPS	RMSE 1 [m^3]	RMSE 10 [m^3]
B1a	69%	30%	131.9	10.8	247.9
B1b	72%	30%	127.7	10.7	234.1
B2a	68%	29%	126.8	10.7	231.4
B2b	70%	30%	126.0	10.7	230.1
B3a	59%	23%	133.0	10.7	235.5
B3b	64%	27%	128.7	10.6	234.8

593

594 Table 3. Forecast evaluation for mean areal rainfall (type a) and distributed
 595 subcatchment (type c) models with different rainfall inputs for the Damhusåen
 596 catchment (D). Values are based on predicted runoff volumes in m^3 over a prediction
 597 horizon of 100 min (10 time steps) and averaged over the considered rain events. We
 598 include RMSE values for 1-step and 10-step prediction horizons.

Model	Rel [%]	ARIL [%]	CRPS	RMSE 1 [m^3]	RMSE 10 [m^3]
D1a	66%	35%	1126.3	61.2	2864.1
D1c	51%	20%	1029.5	46.9	2112.9
D2a	53%	23%	1210.6	70.2	2330.2

D2c	51%	22%	962.6	45.1	1900.9
D3a	51%	21%	1262.5	70.9	2416.0
D3c	52%	21%	1133.4	47.3	2301.3

599

600 Evaluating the probabilistic runoff forecast skill obtained for the different events
601 (Figure 9), we see that the event with the highest volume and rain intensity (no. 6,
602 c.f. Figure 4 and Figure 6) also leads to rather high forecast errors. We cannot
603 identify a clear relation between event characteristics (Figure 4) and runoff forecast
604 qualities which may be due to the small number of events considered. For event 2 the
605 clearly lowest forecasting skill in the Ballerup catchment is observed when using rain
606 gauge input which is a result of the gauges being located outside the catchment as
607 discussed earlier.

608

609 FIGURE 8 APPROX. HERE

610

611 FIGURE 9 APPROX. HERE

612

613 3.4 PROBABILISTIC RUNOFF FORECASTING WITH DIFFERENT SPATIAL

614 RESOLUTIONS

615 Comparing model layouts that account for the spatial distribution of rainfall
616 observations in different degrees of detail, we can identify a trend that smaller
617 forecast errors are obtained with more complex model structures.
618 Table 2 compares the runoff forecasting skills in the Ballerup catchment. For all
619 rainfall inputs, slightly smaller *CRPS* and *RMSE* values are obtained on the 10-step
620 horizon for the integrated subcatchment approach (model type b). The estimation of a

621 separate effective area and using different rainfall inputs for each subcatchment,
622 instead of averaging all inputs into a mean areal rainfall, consequently yields better
623 results.

624

625 A similar trend can be observed in the Damhusåen catchment (Table 3). Accounting
626 for the spatial rainfall distribution with a more complex model structure (distributed
627 subcatchment approach - model type c) leads to a clear reduction in forecast error for
628 all rainfall inputs. Following the discussion in Schilling and Fuchs (1986), this result
629 was expected. Also with the slightly more complex model structure, models with
630 statically adjusted radar input outperform those with rain gauge input and
631 dynamically adjusted radar input (comparing models D1c, D2c and D3c in terms of
632 *CRPS* and *RMSE*).

633

634 **4 CONCLUSIONS**

635 The quality of probabilistic on-line runoff forecasts obtained with different types of
636 rainfall input and different conceptual model layouts that account for the spatial
637 distribution of rainfall in varying degrees of detail was analysed. Forecasts were
638 generated for two urban catchments with forecast horizons of up to 100 min. A
639 number of conclusions were identified with respect to the considerations described in
640 section 1. These are summarized here.

641

642 1) The time-dynamic adjustment of radar observations to rain gauges that is applied
643 here makes those data resemble the rain gauge observations more closely.

644

645 2) Radar rainfall observations and forecasts can improve the skill of probabilistic
646 runoff forecasts compared with those based on rain gauges.

647

648 3) For all considered runoff model structures, the best results are obtained with radar
649 input that is time-statically adjusted to rain gauge observations. The time varying
650 (dynamic) adjustment of the radar data reduces the potential for creating runoff
651 forecasts with the stochastic grey box models. In fact, also the cross correlation
652 between radar rainfall and runoff measurements is reduced as a result of the time
653 varying radar adjustment.

654

655 4) Rainfall inputs for conceptual, data-driven forecasting models need not be the
656 same as the values observed by gauges on the ground. The model can to some extent
657 adapt to the characteristics of the input series in the parameter estimation procedure
658 and will give the best forecasts with the rainfall input that best explains the patterns
659 in the flow observations. In this sense, the radar is likely to provide a better spatial
660 representation of rainfall patterns which, although biased compared with the ground
661 observations, leads to better runoff forecasts. It is, however, important that the bias of
662 the radar observations is not altered in a non-constant fashion. The aim of the radar
663 adjustment should in this context be to merge rainfall information from different
664 sources in a statistically optimal way.

665

666 5) An evaluation of radar adjustment methodologies should not only focus on the
667 comparison with rain gauge observations but also on the final purpose for the
668 adjusted measurements. In our case, this was runoff forecasting with data-driven

669 models and the radar adjustment and the runoff forecasting models should
670 consequently be considered as a chain and coordinated.

671

672 6) Generally, rainfall runoff forecasting models will yield best results if the applied
673 rainfall input closely resembles the input used in model calibration. Distributed
674 simulation models are typically calibrated to resemble observations in the sewer
675 network based on rain gauge observations. Adjusting radar data to more closely
676 resemble the observations of rain gauges will consequently improve the results
677 obtained with these models. Any type of model calibrated using radar rainfall
678 observations as input may, however, yield different results.

679

680 7) The probabilistic runoff forecasts obtained with the stochastic grey-box models
681 improve if we account for the spatial distribution of rainfall in the model. The best
682 forecasts in the Damhusåen catchment are obtained for the distributed subcatchment
683 approach, i.e. when splitting the catchment into 3 subcatchments that are modelled
684 by separate, connected reservoir cascades.

685

686 8) We can identify insufficiencies in the applied models. The uncertainty description
687 based on the model states does not allow us to capture the high forecast uncertainty
688 at the start of a rain event. An improved model layout should be obtained by making
689 the model uncertainty depend on the rainfall input. Further, considering also dry
690 weather periods during parameter estimation of the models leads to unacceptably
691 small uncertainty estimates during rain events. Either, only periods with rainfall
692 should be considered for parameter estimation, or the model structure should be

693 modified to allow for proper separation between forecast uncertainties during dry and
694 wet weather.

695

696 **5 ACKNOWLEDGEMENTS**

697

698 This research has been financially supported by the Danish Council for Strategic
699 Research, Programme Commission on Sustainable Energy and Environment through
700 the Storm- and Wastewater Informatics (SWI) project. The catchment and flow data
701 were kindly provided by Avedøre Wastewater Services and Copenhagen Utility
702 Company (HOFOR). We thank the Danish Weather Service (DMI) for providing
703 data from the C-Band radar at Stevns.

704

705 **6 REFERENCES**

706 Achleitner, S., Möderl, M., Rauch, W., 2007. CITY DRAIN © – An open source
707 approach for simulation of integrated urban drainage systems. Environ. Model.
708 Softw. 22, 1184–1195.

709

710 Achleitner, S., Fach, S., Einfalt, T., Rauch, W., 2009. Nowcasting of rainfall and of
711 combined sewage flow in urban drainage systems. Water Sci Technol 59, 1145-1151.

712

713 Berne, A., Delrieu, G., Creutin, J.D., Obled, C., 2004. Temporal and spatial
714 resolution of rainfall measurements required for urban hydrology. J Hydrol 299, 166-
715 179.

716

- 717 Borup, M., Grum, M., Linde, J. J., Mikkelsen, P. S., 2009. Application of high
718 resolution x-band radar data for urban runoff modelling: constant vs. dynamic
719 calibration, 8th International Workshop on Precipitation in Urban Areas, 10-13
720 December, 2009, St. Moritz, Switzerland.
721
- 722 Breinholt, A., Thordarson, F.O., Møller, J.K., Grum, M., Mikkelsen, P.S., Madsen,
723 H., 2011. Grey-box modelling of flow in sewer systems with state-dependent
724 diffusion. *Environmetrics* 22, 946-961.
725
- 726 Breinholt, A., Møller, J.K., Madsen, H., Mikkelsen, P.S., 2012. A formal statistical
727 approach to representing uncertainty in rainfall-runoff modelling with focus on
728 residual analysis and probabilistic output evaluation - distinguishing simulation and
729 prediction, *J Hydrol*, 472-473, 36-52.
730
- 731 Breinholt, A., Grum, M., Madsen, H., Thordarson, F.Ö., Mikkelsen, P.S., 2013.
732 Informal uncertainty analysis (GLUE) of continuous flow simulation in a hybrid
733 sewer system with Infiltration Inflow – consistency of containment ratios in
734 calibration and validation? *Hydrol Earth Syst Sci.* 17, 4159-4176
735
- 736 Brown, P.E., Diggle, P.J., Lord, M.E., Young, P.C., 2001. Space-time calibration of
737 radar rainfall data. *J Roy Stat Soc C-App* 50, 221-241.
738
- 739 Cole, S.J., Moore, R.J., 2008. Hydrological modelling using raingauge- and radar-
740 based estimators of areal rainfall. *J Hydrol* 358, 159-181.

741

742 Chumchean, S., Seed, A., Sharma, A., 2006. Correcting of real-time radar rainfall
743 bias using a Kalman filtering approach. *J Hydrol* 317, 123.

744

745 Das, T., Bárdossy, A., Zehe, E., He, Y., 2008. Comparison of conceptual model
746 performance using different representations of spatial variability. *J Hydrol* 356, 106-
747 118.

748

749 Del Giudice, D., Honti, M., Scheidegger, A., Albert, C., Reichert, P., Rieckermann,
750 J., 2013. Improving uncertainty estimation in urban hydrological modeling by
751 statistically describing bias. *Hydrol Earth Syst Sci Discuss*, 10, 5121–5167.

752

753 Dotto, C.B.S., Mannina, G., Kleidorfer, M., Vezzaro, L., Henrichs, M., McCarthy,
754 D.T., Freni, G., Rauch, W., Deletic, A., 2012. Comparison of different uncertainty
755 techniques in urban stormwater quantity and quality modelling. *Water Res* 46, 2545–
756 58.

757

758 Einfalt, T., Denoeux, T., Jacquet, G., 1990. A radar rainfall forecasting method
759 designed for hydrological purposes. *J Hydrol* 114, 229-244.

760

761 Einfalt, T., Arnbjerg-Nielsen, K., Golz, C., Jensen, N., Quirnbach, M., Vaes, G.,
762 Vieux, B., 2004. Towards a roadmap for use of radar rainfall data in urban drainage.
763 *J Hydrol* 299, 186-202.

764

765 Emmanuel, I., Andrieu, H., Tabary, P., 2012a. Evaluation of the new French
766 operational weather radar product for the field of urban hydrology. *Atmos Res* 103,
767 20-32.
768
769 Emmanuel, I., Andrieu, H., Leblois, E., Flahaut, B., 2012b. Temporal and spatial
770 variability of rainfall at the urban hydrological scale. *J Hydrol* 430, 162-172.
771
772 Fuchs, L., Beeneken, T., 2005. Development and implementation of a real-time
773 control strategy for the sewer system of the city of Vienna. *Water Sci Technol* 52,
774 187-194.
775
776 Giebel, G., Brownsword, R., Karioniotakis, G., Denhard, M., Draxl, C., 2011. The
777 State-Of-The-Art in Short-Term Prediction of Wind Power - A Literature Overview.
778 FP6 ANEMOS.plus deliverable.
779
780 Gill, R. S., Overgaard, S., Bøvith, T., 2006. The Danish weather radar network, 4th
781 European Conference on Radar in Meteorology and Hydrology, 18-22 September,
782 2006, Barcelona, Spain.
783
784 Gjertsen, U., Salek, M., Michelson, D.B., 2003. Gauge-adjustment of radar-based
785 precipitation estimates—a review. COST-717 Work. Doc. WDD 2.200310.
786

787 Gneiting, T., Raftery, A.E., Westveld III, A.H., Goldman, T., 2005. Calibrated
788 probabilistic forecasting using ensemble model output statistics and minimum CRPS
789 estimation. *Mon Weather Rev* 133, 1098-1118.
790
791 Gneiting, T., 2007. Strictly proper scoring rules, prediction, and estimation. *J Am*
792 *Stat Assoc* 102, 359-378.
793
794 Goudenhoofdt, E., Delobbe, L., 2009. Evaluation of radar-gauge merging methods
795 for quantitative precipitation estimates. *Hydrol Earth Syst Sci* 13, 195-203.
796
797 Gourley, J.J., Vieux, B.E., 2005. A Method for Evaluating the Accuracy of
798 Quantitative Precipitation Estimates from a Hydrologic Modeling Perspective. *J*
799 *Hydrometeorol* 6, 115–133.
800
801 Grum, M., Thornberg, D., Christensen, M.L., Shididi, S.A., Thirsing, C., 2011. Full-
802 Scale Real Time Control Demonstration Project in Copenhagen's Largest Urban
803 Drainage Catchments, Proceedings of the 12th International Conference on Urban
804 Drainage, 11-16 Sep, Porto Alegre / Brazil.
805
806 Jin, X., Xu, C.Y., Zhang, Q., Singh, V., 2010. Parameter and modeling uncertainty
807 simulated by GLUE and a formal Bayesian method for a conceptual hydrological
808 model. *J Hydrol* 383, 147-155.
809

- 810 Jørgensen, H.K., Rosenørn, S., Madsen, H., Mikkelsen, P.S., 1998. Quality control of
811 rain data used for urban runoff systems. *Water Sci Technol* 37(11), 113-120.
- 812
- 813 Kloeden, P.E., Platen, E., 1999. Numerical Solution of Stochastic Differential
814 Equations. third ed., Springer, Berlin-Heidelberg-New York.
- 815
- 816 Kraemer, S., Grum, M., Verworn, H.R., Redder, A., 2005. Runoff modelling using
817 radar data and flow measurements in a stochastic state space approach. *Water Sci*
818 *Technol* 52, 1-8.
- 819
- 820 Kristensen N.R., Madsen H., 2003. Continuous time stochastic modelling CTSM -
821 mathematics guide. Technical report, Technical University of Denmark, URL
822 <http://CTSM.info>.
- 823
- 824 Kristensen, N.R., Madsen, H., Jørgensen, S.B., 2004. Parameter estimation in
825 stochastic grey-box models. *Automatica* 40, 225–237.
- 826
- 827 Kuczera, G., Kavetski, D., Franks, S., Thyer, M., 2006. Towards a Bayesian total
828 error analysis of conceptual rainfall-runoff models: Characterising model error using
829 storm-dependent parameters, *J Hydrol* 331, 161-177.
- 830
- 831 Löwe, R., Mikkelsen, P., Madsen, H., 2014. Stochastic rainfall-runoff forecasting:
832 parameter estimation, multi-step prediction, and evaluation of overflow risk. *Stoch*
833 *Environ Res Risk Assess* 28, 505-516, doi 10.1007/s00477-013-0768-0.

834

835 Nielsen, H.A., Madsen, H., 2006. Modelling the heat consumption in district heating
836 systems using a grey-box approach. *Energy Build* 38, 63–71.

837

838 Nielsen, J.E., Thorndahl, S., Rasmussen, M.R., 2014. A numerical method to
839 generate high temporal resolution precipitation time series by combining weather
840 radar measurements with a nowcast model. *Atmos Res* 138, 1–12, doi
841 10.1016/j.atmosres.2013.10.015.

842

843 Pleau, M., Pelletier, G., Lavalle, P., Bonin, R., 2001. Global predictive real-time
844 control of Quebec Urban Communitys westerly sewer network. *Water Sci Technol*
845 43, 123-130.

846

847 Pleau, M., Colas, H., Lavallée, P., Pelletier, G., Bonin, R., 2005. Global optimal real-
848 time control of the Quebec urban drainage system. *Environ Modell Softw* 20, 401-
849 413.

850

851 Puig, V., Cembrano, G.G., Romera, J., Quevedo, J., Aznar, B., Ramón, G., Cabot, J.,
852 2009. Predictive optimal control of sewer networks using CORAL tool: application
853 to Riera Blanca catchment in Barcelona. *Water Sci Technol* 60, 869-878.

854

855 Reed, S., Koren, V., Smith, M., Zhang, Z., Moreda, F., Seo, D., DMIP Participants,
856 2004. Overall distributed model intercomparison project results. *J Hydrol* 298, 27-60.

857

- 858 Renard, B., Kavetski, D., Kuczera, G., Thyer, M., Franks, S., 2010: Understanding
859 predictive uncertainty in hydrologic modeling: The challenge of identifying input
860 and structural errors, *Water Resour Res* 46, W05521.
- 861
- 862 Schellart, A., Shepherd, W., Saul, A., 2011. Influence of rainfall estimation error and
863 spatial variability on sewer flow prediction at a small urban scale. *Adv Water Resour*
864 45, 65-75.
- 865
- 866 Schilling, W., 1984. Effect of spatial rainfall distribution on sewer flows. *Water Sci*
867 *Technol* 16, 177-188.
- 868
- 869 Schilling, W., Fuchs, L., 1986. Errors in stormwater modeling-a quantitative
870 assessment. *J Hydraul Eng* 112, 111-123.
- 871
- 872 Schilling, W., 1991. Rainfall data for urban hydrology: what do we need? *Atmos Res*
873 27, 5-21.
- 874
- 875 Seggelke, K., Löwe, R., Beeneken, T., Fuchs, L., 2013. Implementation of an
876 integrated real-time control system of sewer system and WWTP in the city of
877 Wilhelmshaven. *Urban Water J* 10, 330-341.
- 878
- 879 Sharma, A.K., Guildal, T., Thomsen, H.A.R., Mikkelsen, P.S., Jacobsen, B.N., 2013.
880 Aeration tank settling and real time control as a tool to improve the hydraulic

881 capacity and treatment efficiency during wet weather: results from 7 years' full-scale
882 operational data. *Water Sci Technol* 67, 2169-2176.

883

884 Thordarson, F.O., Breinholt, A., Møller, J.K., Mikkelsen, P.S., Grum, M., Madsen,
885 H., 2012. Uncertainty assessment of flow predictions in sewer systems using grey
886 box models and skill score criterion. *Stoch Env Res Risk A* 26, 1151-1162.

887

888 Thorndahl, S., Beven, K.J., Jensen, J.B., Schaarup-Jensen, K., 2008. Event based
889 uncertainty assessment in urban drainage modeling, applying the GLUE
890 methodology, *J Hydrol* 357, 421-437.

891

892 Thorndahl, S., Rasmussen, M. R., Grum, M., Neve, S. L., 2009. Radar Based Flow
893 and Water Level Forecasting in Sewer Systems: a Danish case study. 8th
894 International Workshop on Precipitation in Urban Areas, 10-13 December, 2009, St.
895 Moritz, Switzerland.

896

897 Thorndahl, S., Rasmussen, M.R., Neve, S., Poulsen, T.S., Grum, M., 2010.
898 Vejrradarbaseret styring af spildevandsanlæg (in Danish). DCE Technical Report No.
899 95, Aalborg Universitet. Institut for Byggeri og Anlæg, ISSN 1901-726X.

900

901 Thorndahl, S., Rasmussen, M.R., 2013. Short-term forecasting of urban storm water
902 runoff in real-time using extrapolated radar rainfall data. *J Hydroinf* 15, 214-226.

903

904 Thorndahl, S., Nielsen, J.E., Rasmussen, M.R., 2014. Bias adjustment and advection
905 interpolation of long-term high resolution radar rainfall series. *J Hydrol* 508, 214-
906 226.

907

908 Tolson, B. A., Shoemaker, C. A., 2007. Dynamically dimensioned search algorithm
909 for computationally efficient watershed model calibration, *Water Resour Res* 43,
910 W01413.

911

912 Vezzaro, L., Grum, M., 2012. A generalized Dynamic Overflow Risk Assessment
913 (DORA) for urban drainage RTC. 9th International Conference on Urban Drainage
914 Modelling, 3-7 September, 2012, Belgrade, Serbia.

915

916 Vieux, B.E., Bedient, P.B., 2004. Assessing urban hydrologic prediction accuracy
917 through event reconstruction. *J Hydrol* 299, 217–236.

918

919 Villarini, G., Smith, J.A., Lynn Baeck, M., Sturdevant-Rees, P., Krajewski, W.F.,
920 2010. Radar analyses of extreme rainfall and flooding in urban drainage basins. *J*
921 *Hydrol* 381, 266-286.

922

923 Wang, L., Ochoa, S., Simões, N., Onof, C., Maksimović, Č., 2013. Radar-raingauge
924 data combination techniques: a revision and analysis of their suitability for urban
925 hydrology. *Water Sci Technol* 68, 737-747.

926

927 Wolfs, V., Villazon, M.F., Willems, P., 2013. Development of a semi-automated
928 model identification and calibration tool for conceptual modelling of sewer systems.
929 Water Sci. Technol. Sci. Technol. 68, 167–175.

930

931 Wood, S.J., Jones, D.A., Moore, R.J., 2000. Static and dynamic calibration of radar
932 data for hydrological use. Hydrol Earth Syst Sci 4, 545–554.

933

934 **7 FIGURE CAPTIONS**

935

936 Figure 1. Ballerup (left) and northern Damhusåen (right) catchments with C-band
937 radar pixels (2x2km), location of rain gauges shown as dots (large grey circles – used
938 in radar adjustment, white rectangles – used as input to Ballerup model, black
939 triangles – used as input to Damhusåen model, small black dots – other gauges).
940 Different radar pixel shadings correspond to different subcatchments (c.f. section
941 2.5.2).

942

943 Figure 2. Areal mean of rain gauge observations and flow measurements for the
944 Ballerup catchment in the estimation period.

945

946 Figure 3. Simulation run identifiers depending on considered catchments, rainfall
947 input and spatial resolution.

948

949 Figure 4. Rain event depths (left) and maximum intensity (right) derived for mean
950 areal rainfall with different rainfall measurements in the Ballerup catchment. Left
951 plot includes label of duration of rain event (in min).

952

953 Figure 5. Sample rainfall event in the Ballerup catchment. Part a: rain gauge
954 observations (black, as in model B1a) and rainfall forecasts with lead times of 20 min
955 (green) and 100 min (blue), Part b: statically adjusted radar rainfall observations and
956 forecasts (B2a), Part c: dynamically adjusted radar rainfall observations and forecasts
957 (B3a).

958

959 Figure 6. Total forecasted (FC) rainfall amount for the Ballerup catchment for lead
960 times of 20 (left) and 100min (right) for the considered rain events, together with
961 rainfall amount observed by rain gauges.

962

963 Figure 7. Cross correlation (CCF) between runoff and catchment averaged rainfall
964 observations in the Ballerup catchment. Rainfall observations are lagged in 10min
965 steps to the runoff observations.

966

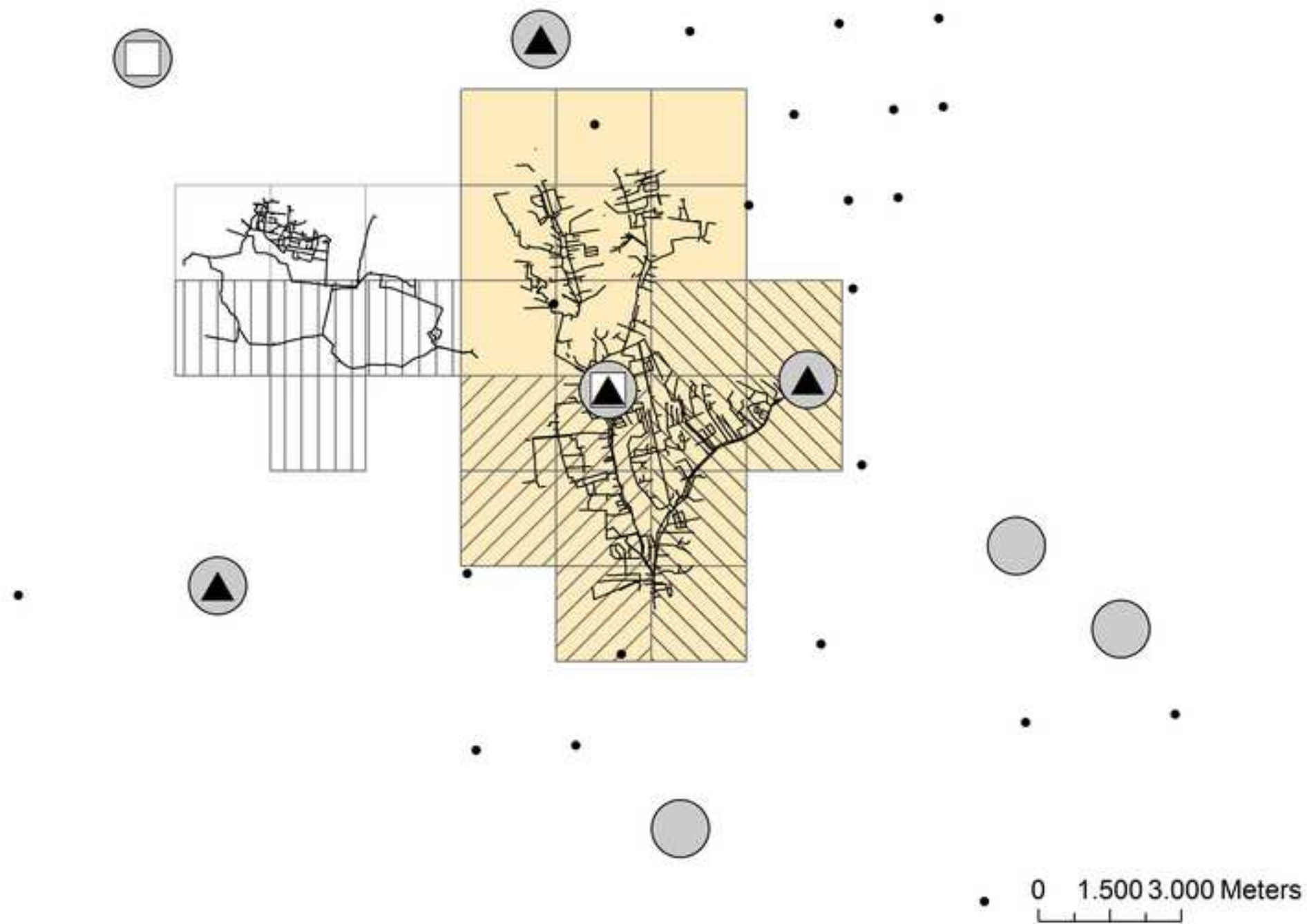
967 Figure 8. 10-step forecasts of runoff volume for event 6 in Ballerup (left, model B2a)
968 and Damhusåen (right, model D2a) catchments together with observation (red). The
969 shading corresponds to different prediction intervals with coverage rates from 2% to
970 98%.

971

972 Figure 9. Quality of probabilistic runoff forecasts for 100 min horizon (10 step)
973 expressed as CRPS for different rain events and inputs in Ballerup (left) and
974 Damhusåen (right) catchments.

975

Figure1



AC

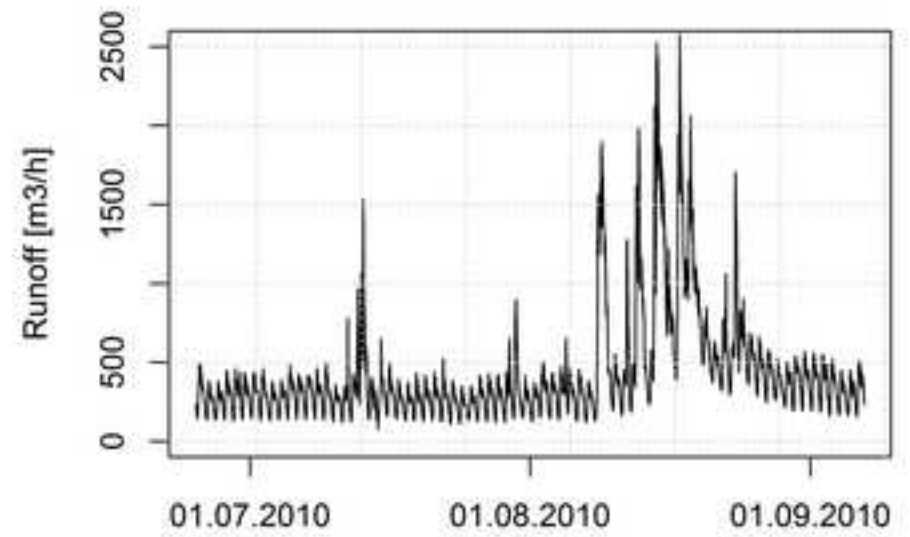
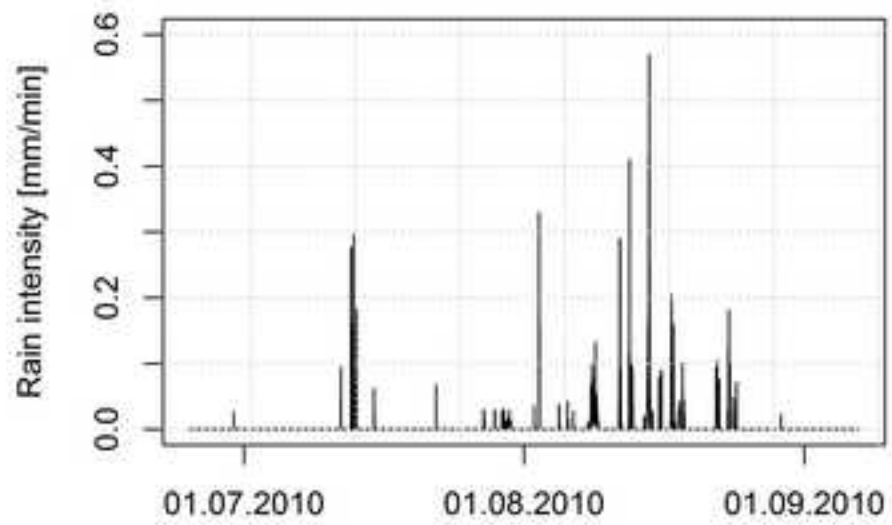
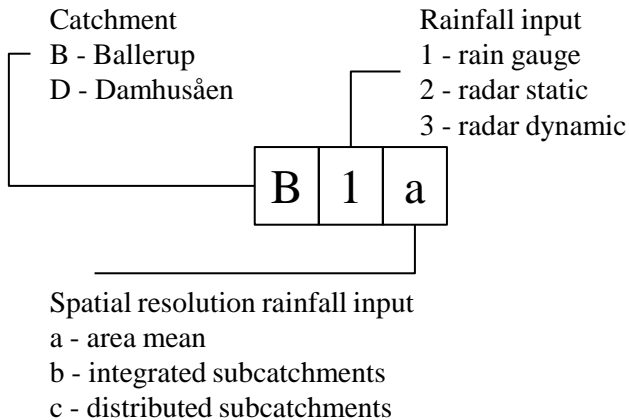
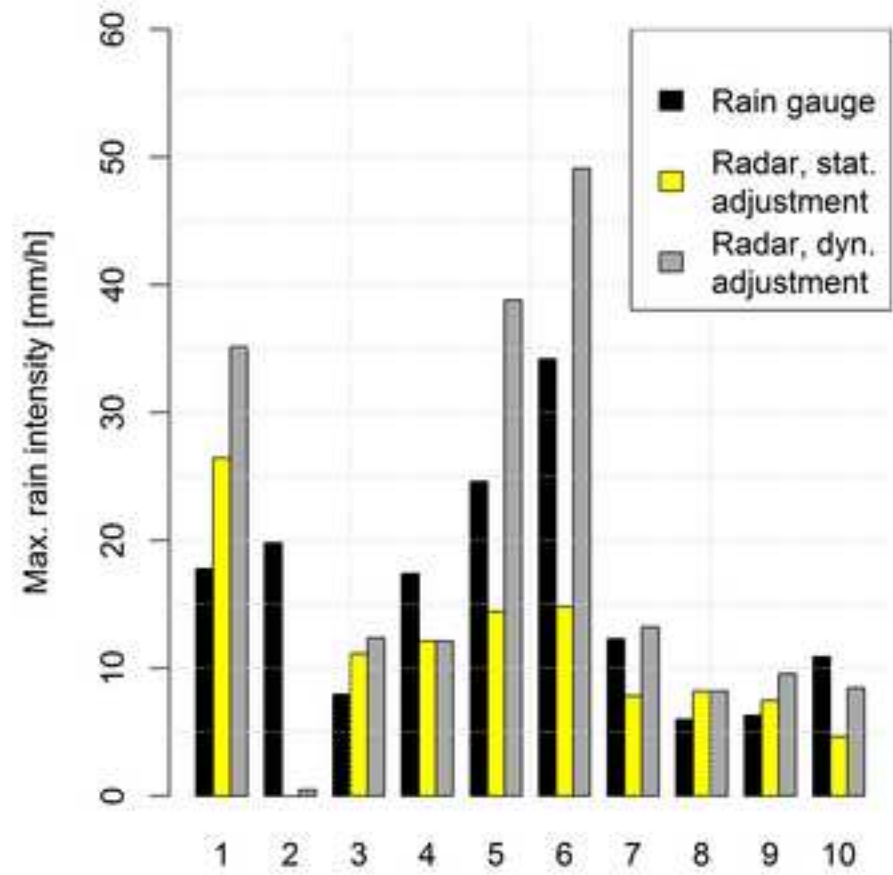
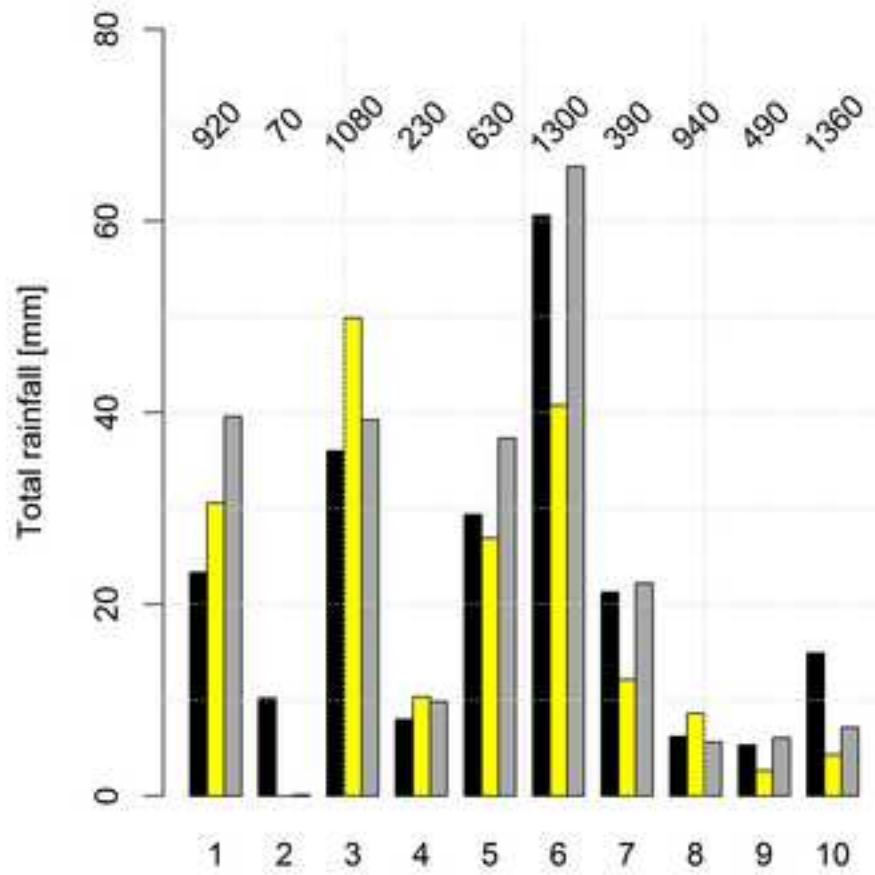
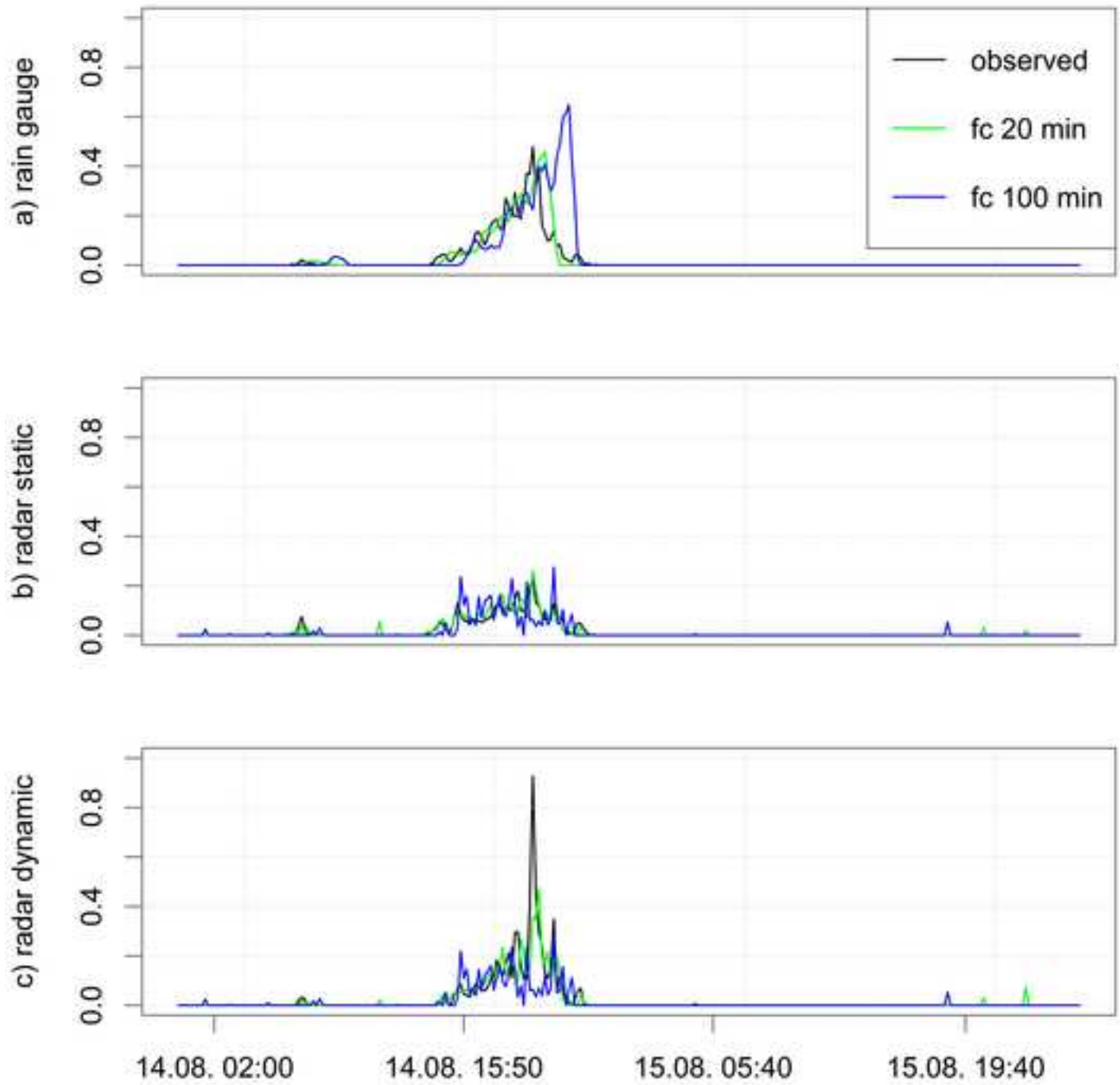
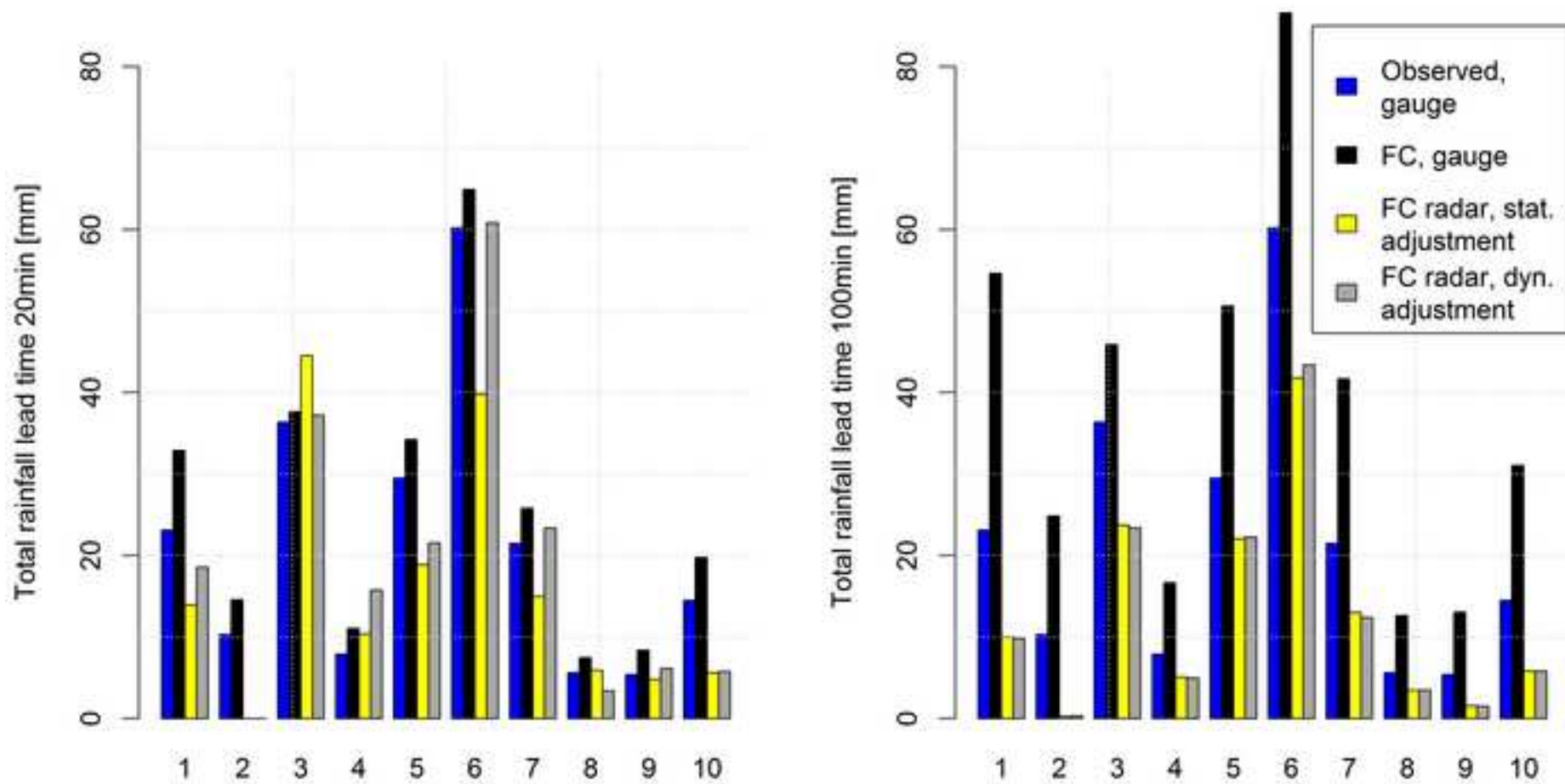


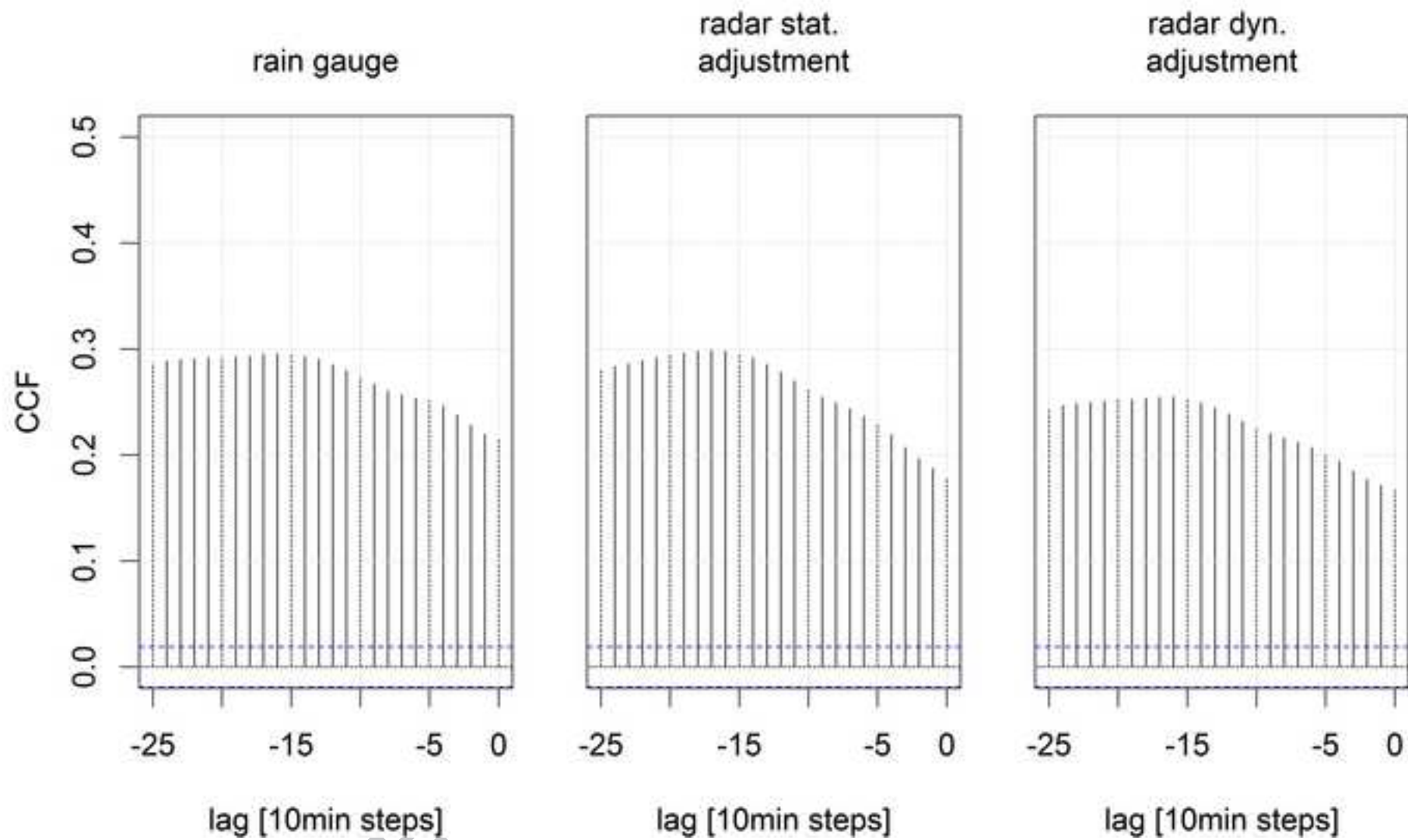
Figure3

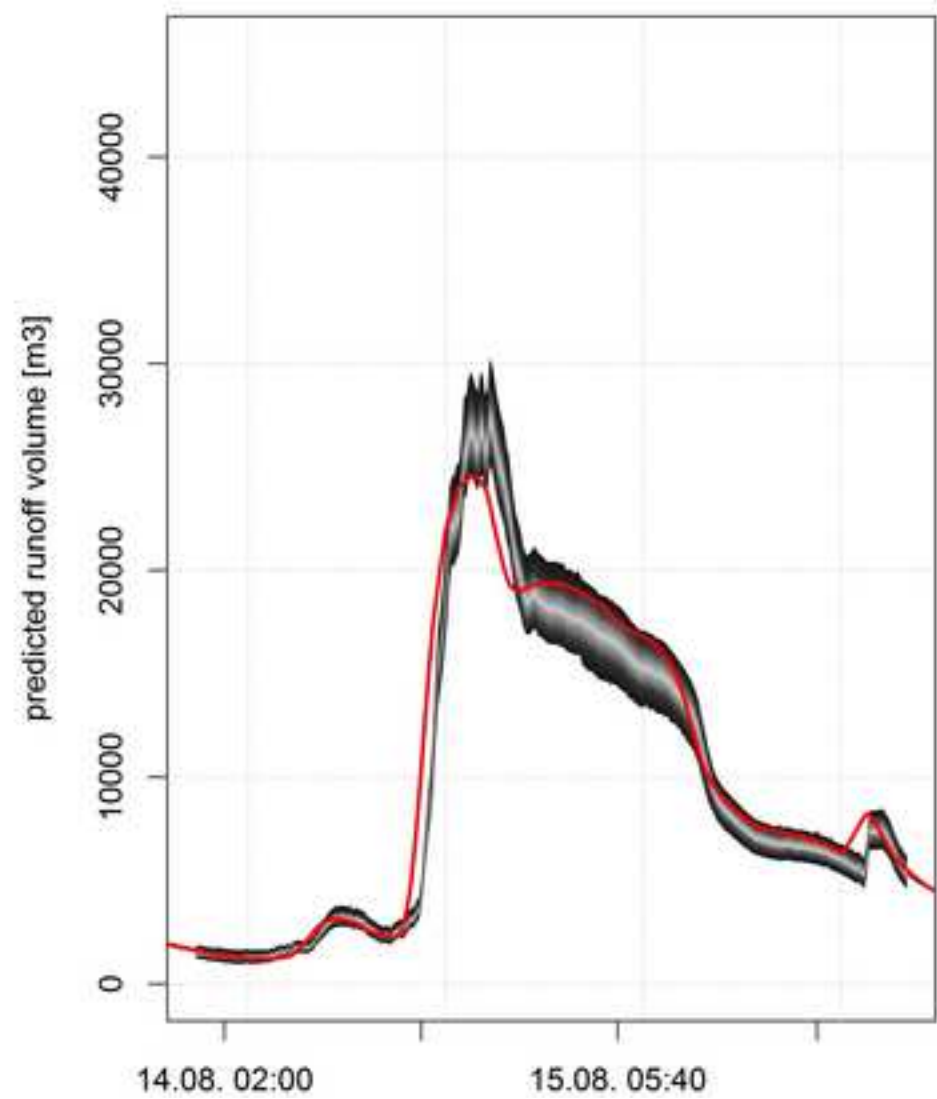
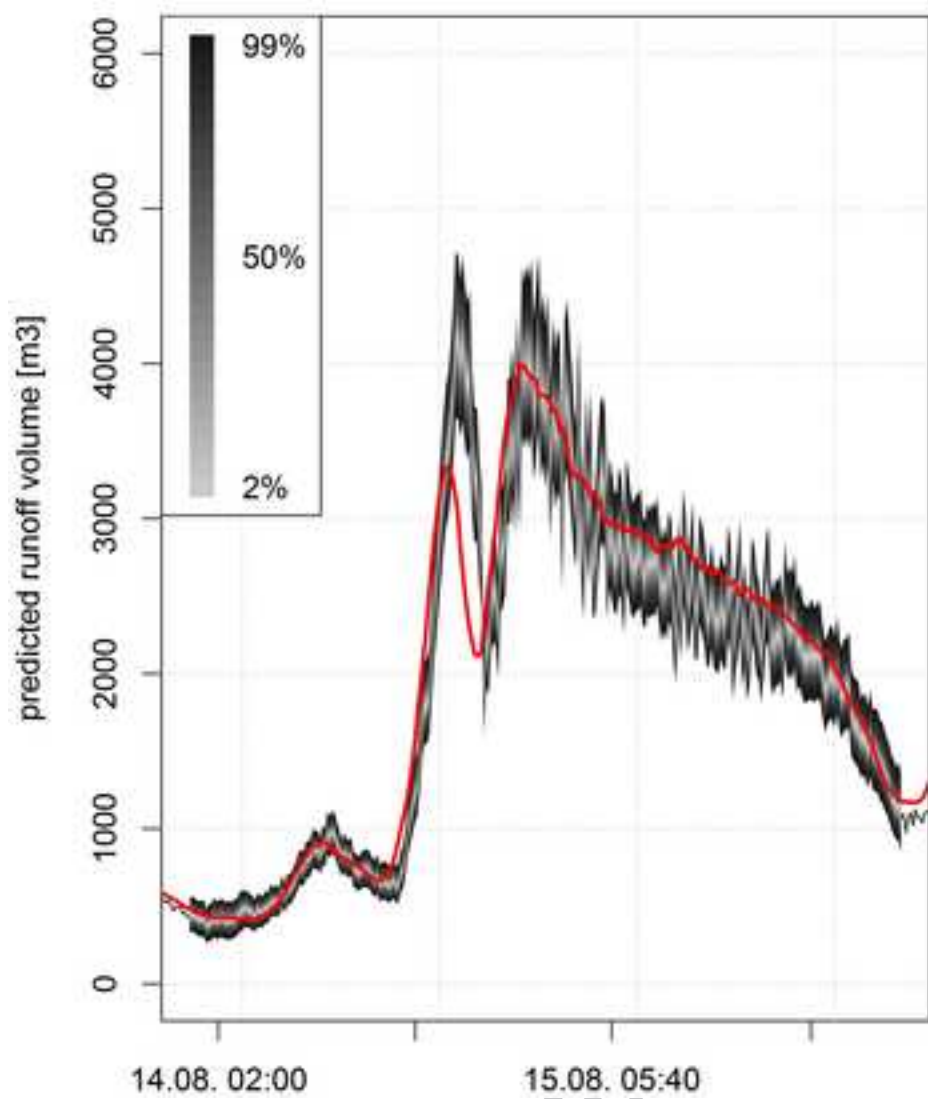


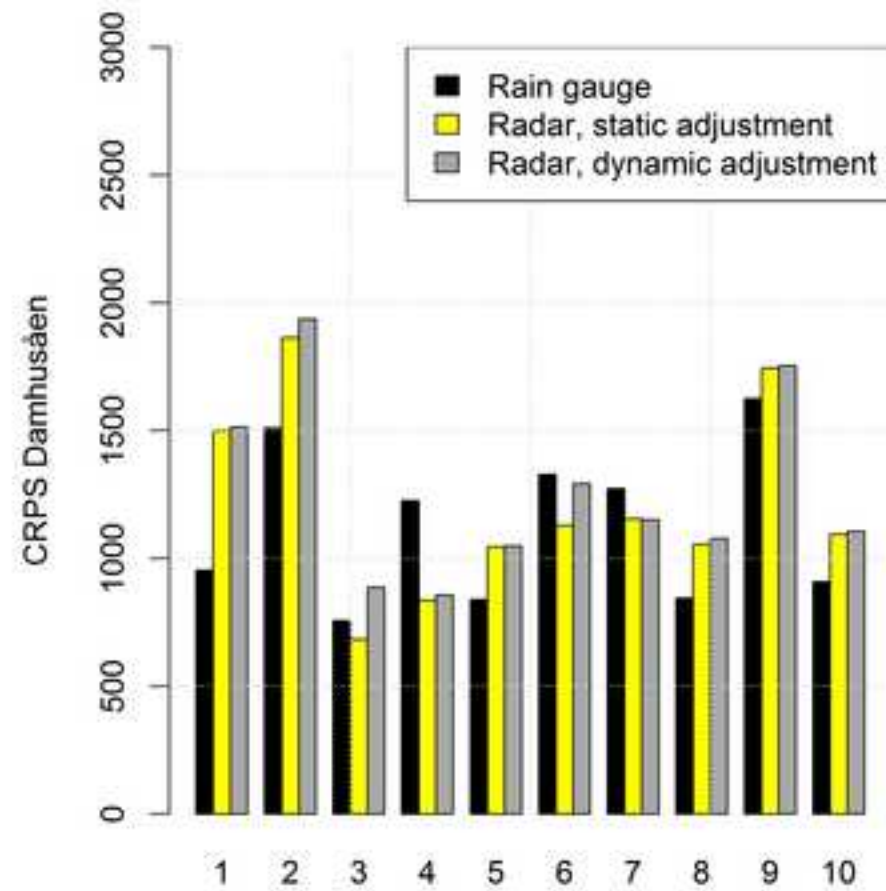
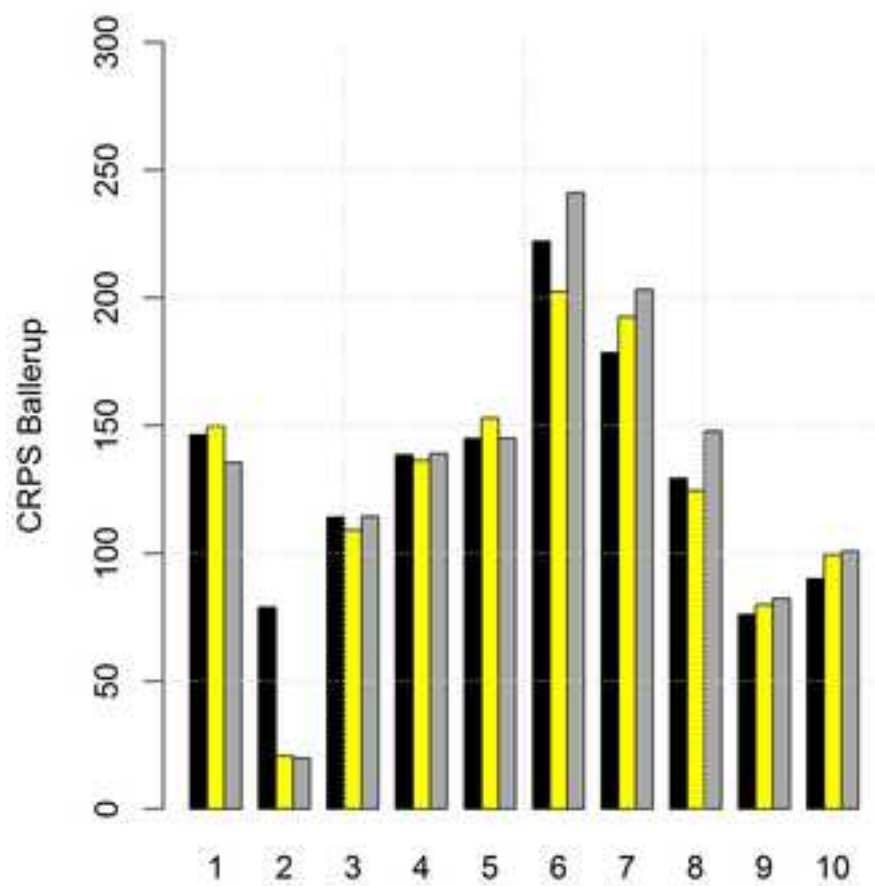












976 **8 HIGHLIGHTS**

977

- 978 • Rainfall nowcasts from rain gauges and 2 types of adjusted radar data are
979 compared
- 980 • Probabilistic runoff forecasts are generated in 2 urban catchments in an on-
981 line mode
- 982 • Time-statically adjusted radar data as model input yield best runoff forecasts
- 983 • Radar adjustment and online runoff forecast should be considered as a whole
- 984 • Improved spatial resolution in on-line rainfall runoff models improves
985 forecasts

986

ACCEPTED MANUSCRIPT